# Numerical Analysis of Threaded Pin Fins Heat Sink by Natural Convection

*Muhammad Firdaus Hamidan, Rosnadiah Bahsan*[*]*, Alhassan Salami Tijani, Irnie Azlin Zakaria*
*School of Mechanical Engineering, College of Engineering, Universiti Teknologi MARA, 40450 Shah Alam, Selangor, MALAYSIA*
[*]*rosnadiah@uitm.edu.my*

*Sajith Thottathil Abdulrahman*
*Department of Mechanical Engineering, KMEA Engineering College, 683560 Edathala P.O., Cochin, INDIA*

ABSTRACT

*Heat sinks play a crucial role in thermal management by dissipating heat away from electronic devices and reducing the device's performance. The heat sink with pin fins will enhance the rate of convective heat transfer and improve the cooling efficiency of electronic components by increasing the surface area. This study investigates the enhancement of heat transfer rate on square threaded pin fin heat sinks with or without perforation under natural convection. The fins were arranged in inline and staggered arrangement. Four different configurations were designed by using CATIA V5 and simulated by using CFD analysis with different power inputs at 5 W, 10 W and 15 W. The simulation results were validated with the experimental results from the previous study by comparing the heat transfer coefficient of the heat sink design by natural convection. The results show that the average heat transfer coefficient of square threaded pin fins with perforations in staggered arrangement is 7.365 W/m$^2$.$^o$C compared to the pin fins without perforations which is 7.168 W/m$^2$.$^o$C. Therefore, pin fin with perforation dissipates heat at the rate of 2.75% more than pin fin without perforation. In conclusion, the square threaded pin fins with perforations in staggered arrangement have higher heat transfer performance.*

**Keywords:** *Computational Fluid Dynamics (CFD); Heat Transfer Coefficient; Natural Convection; Nusselt Number; Square Thread Pin Fins, Perforation*

ISSN 1823-5514, eISSN 2550-164X

https://doi.org/10.24191/jmeche.v12i1.24645

Received for review: 2023-10-03
Accepted for publication: 2023-10-22
Published: 2023-11-15

## Introduction

Innovation in electronic device products such as smartphones, computers and electrical appliances will evolve towards miniaturization [1]. The electronic appliances are going into miniaturization in which the size of the device will be minimised to a small dimension which means the space for the cooling system is limited. The small size of the heat sink will reduce its surface area and can reduce its efficiency in a cooling system [2]. The temperature rise in electronic devices is perpendicular to the increasing chance of malfunctioning the device [3].

Effective thermal management in electronic devices is vital for maximising the performance, dependability, and lifespan, especially for high-performance devices such as gaming laptops, which consume a very high amount of electricity due to the large amount of data processed by the computer at a times causing greater heat generation. As technology progresses, the demand for innovative thermal management solutions grows. Inefficient heat transfer by the heat sink may cause a large thermal concentration within the body, which may cause the electronic devices to degrade [4]. Advancements and improvements are required in the field of cooling systems in order to meet the requirements for heat sink efficacy.

Heat sinks play a crucial role in electronic devices by dissipating excess heat generated during the operation to the surroundings as much as possible to avoid any malfunction of the system. Convection is widely used to dissipate heat through a medium in thermal management. This is the mode of heat transfer in thermal management through the movement of a fluid caused by the differences in temperature within the fluid. This movement can occur naturally (natural convection) or be induced by external means (forced convection). Natural convection known as a passive cooling system relies solely on buoyancy forces created by the variation in fluid density [5]. Natural convection is essential for designing heat sinks that can effectively dissipate heat without the need for additional power-consuming components.

In contrast, forced convection known as an active cooling system relies on the mechanical or electrical propulsion of fluid over a solid surface by mechanical or electrical devices. Enhancing the rate of cooling by using a mechanical device like a fan can increase the electrical power consumption. Although an active cooling system is more efficient in transferring heat than a passive cooling system, it consumes more energy, produces noise and is less reliable due to external devices deteriorating over time such as fans or pumps [6]. Thus, natural convection is often preferred for its simplicity, high reliability and energy efficiency [7].

To augment heat exchange efficiency, fins are employed to increase the available surface area for heat transfer processes. Numerous studies have explored various aspects of fin array and surface texture to enhance heat transfer rate. Nada et al. [8] investigated the effects of fin geometries,

arrangements, dimensions and number of fins on heat transfer due to natural convection. The author found that as the number of fins increased, the effective thermal conductivity improved. Additional perforation on the fin surfaces also demonstrated an increase in surface area which can dissipate more heat to the surrounding. In the fluid flow characteristic, the presence of perforation or hole creates a vortex along the perforation area which then allows more mixing air [9]. Reduces of the weight of the pin fin by perforation contribute to the economic design. The higher number of perforations with a smaller perforation radius is effective in enhancing the heat dissipation rate [10]. MOORA and entropy minimization methods to predict the performance of perforation fin in an inline and staggered arrangement were used by Maji et al. [11]. The result showed that lower velocities from 4 to 6 m/s elliptical perforation on linearly arranged circular fin have a higher heat dissipation against lower pressure loss. Furthermore, obstruction in fluid flow is more in staggered fin than linear fin which causes a higher pressure drop [11].

Laad et al. [12] studied the effect of pin-fin shape on the performance of the heat sink with different shapes of fins such as rectangular, trapezoidal, circular and square. The result showed that the circular pin fins have better performance than the others. An experiment to analyse the performance of fin efficiency by using different materials showed that copper material achieves 94% efficiency in thermal conductivity better than brass and aluminium with 66% and 91% efficiency, respectively [13]. The heat transfer rate in square threaded pin fin with perforations in a staggered arrangement is higher among each other arrangements in natural convection due to obstruction, more circulation, irregularity, and zigzag positions of pin fins in the array which leads to an increase in Reynolds number and Nusselt number of airflow along the pin fin array [14].

All the heat sinks with perforated solid threaded pin fins inline have a higher rate of heat transfer capacity than the other hollow pin fins [15]. The heat transfer rate of square-threaded pin fins with perforations shows the highest rate due to the obstruction in the arrangement of pin fins [16]. Despite these advancements, there exists a notable research gap when it comes to exploring alterations in surface texture such as threading and in the context of thermal management. While fin geometries have been extensively studied, there is limited research on modifying the surface with thread, perforation or additional surface coating [17]. These alterations could potentially offer innovative solutions for enhancing heat dissipation in miniaturized electronic devices. Threaded pin fins represent a specialized design variation of traditional heat sink fins. These fins are characterized by their unique geometry, featuring helical threads that spiral around the fin's central axis. The introduction of threaded pin fins disrupts the thermal boundary layer near the surface of the fin, leading to improved convective heat transfer. This disruption

enhances fluid mixing, increases heat exchange surface area, and reduces thermal resistance, resulting in more efficient heat dissipation.

Therefore, the purpose of this project is to investigate the enhancement of thermal performance through square threaded pin fins with and without perforation of the heat sink with variations of arrangement under natural convection conditions. All heat sink models were simulated using CFD Ansys to observe the flow fields and heat sink performance. Thermal characteristics of the heat sink such as Nusselt number, Rayleigh number, Prandtl number and heat transfer coefficient were analysed.

## Methodology

### Design specification

Threaded pin fins heat sinks were designed using SOLIDWORKS software. Figures 1 and 2 show the square threaded pin fin heat sink without perforation in inline and staggered arrangement. Figures 3 and 4 show the square threaded pin fin heat sink with perforation dimensions. The arrangements of the pin fin were in inline and staggered form. The cross-sectional area for the base plate was 250 mm in length, 125 mm in width and a thickness of 5 mm [16].

Table 1 shows the detailed specification dimensions of the geometry for each heat sink model. Figures 5 and 6 show the detailed dimensions of inline and staggered pattern heat sink. Aluminium was chosen as the material for the pin fins due to its cost effectiveness [18], ease of machining, corrosion-resistant and good thermal conductivity [19]. These characteristics make aluminium a suitable material for heat sink applications.

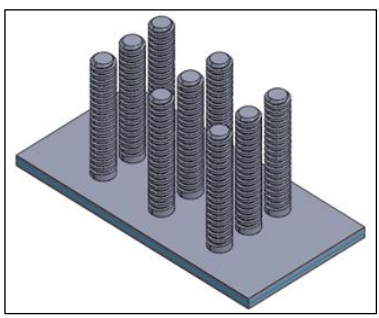

Figure 1: Square threaded pin fin without perforation in inline arrangement

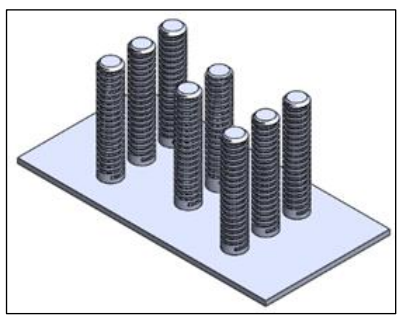

Figure 2: Square threaded pin fin without perforation in a staggered arrangement

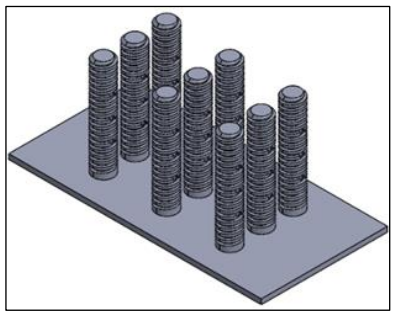

Figure 3: Square threaded pin fin with perforation in inline arrangement

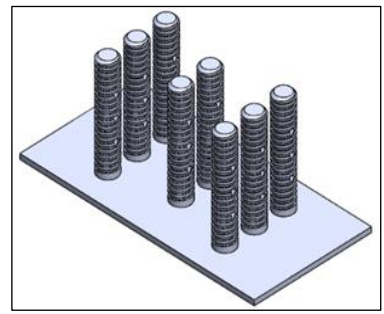

Figure 4: Square threaded pin fin with perforation in a staggered arrangement

Table 1: Dimension for the geometry of the heat sink model

| Type of pin fins | Inline | Inline pattern | Staggered | Staggered |
|---|---|---|---|---|
| Base plate, (mm) | | 250 x 125 x 5 | | |
| Pin height (mm) | 100 | 100 | 100 | 100 |
| Pin outer | 20 | 20 | 20 | 20 |
| Pin inner | 15 | 15 | 15 | 15 |
| Pitch (mm) | 5 | 5 | 5 | 5 |
| Number of pins | 9 | 9 | 8 | 8 |
| Number of | - | 27 | - | 27 |

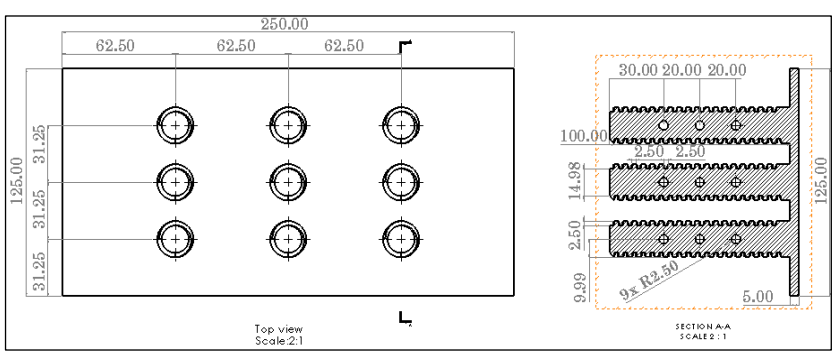


Figure 5: Dimension of pin fins in inline pattern

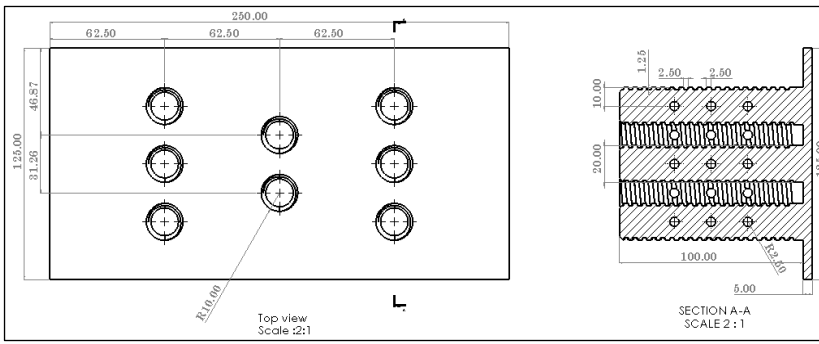


Figure 6: Dimension of pin fins heat sink in a staggered array

## CFD analysis

In this project, steady-state conditions and heat transfer distribution on the heat sink were simulated using the CFD tool of Ansys CFX 2023. The computational domain of the heat sink models was simulated under natural convection conditions in which hot fluid at the bottom of the heat sink was raised and cold air came in the places of hot air. The direction of fluid flow in natural convection was raised against gravitational force. The size of the domain was 300 x 300 x 300 mm. Figure 7 shows the heat sink in the domain.

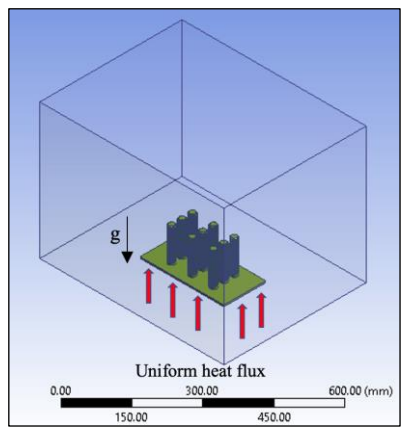


Figure 7: Heat sink in the domain

### Simulation setup and boundary conditions

The modelling of CFD simulation and post-processor was carried out in the ANSYS 2023 R1 workbench using the aid of CFX. Based on a previous study on natural convection, [20] described that ANSYS CFX has the capability of

solving the convective transport of energy by fluid flow and solving thermal conduction in solids. Table 2 shows the overall boundary condition used in this project.

Table 2: Summary of boundary conditions

| Physical condition | |
|---|---|
| Fluid | Steady and incompressible air |
| Fluid volume (L x W x H) | 0.3 x 0.3 x 0.3 m |
| Fin and base heat sink material | Aluminium |
| *Thermal boundary condition* | |
| Air temperature | 25 ℃ |
| Air pressure | 1 atm |
| Heat flux | 480 $W/m^2$ |
| *Computational elements* | |
| Element type | Tetrahedron |
| Number of elements | 3 M elements |
| *Solution model* | |
| Turbulence models | Laminar |
| Analysis type | Steady state |

In this analysis, the enclosure was modelled as a fluid domain and the heat sink was modelled as a solid domain with a supply of heat source from 5 W to 15 W. The analysis was conducted at an atmospheric temperature of 298 K. Boundary conditions were applied as follows:

- Domain interface - The interface between solid fin surface and fluid
- Basic setting - “fluid-solid” interface
- Activated buoyancy in Y-direction, -9.81 $m/s^2$
- Opening - all sides of fluid domain except bottom face
- The bottom face of the fluid domain is set for adiabatic
- The base of the heat sink is set as heat flux.

The whole geometry model was discretized into finite volumes of tetrahedral mesh using suitable mesh. Figures 8 to 11 show the details of the mesh geometry of the heat sink.

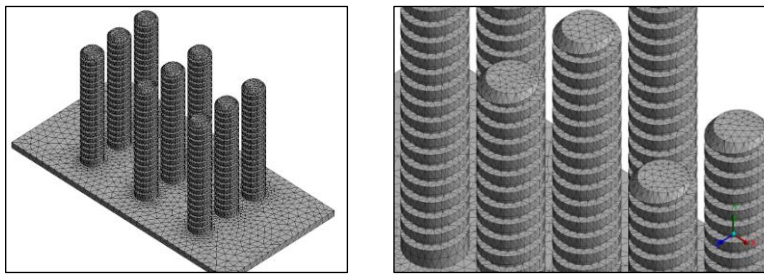

Figure 8: Meshing view of square threaded pin fin without perforation in inline arrangement

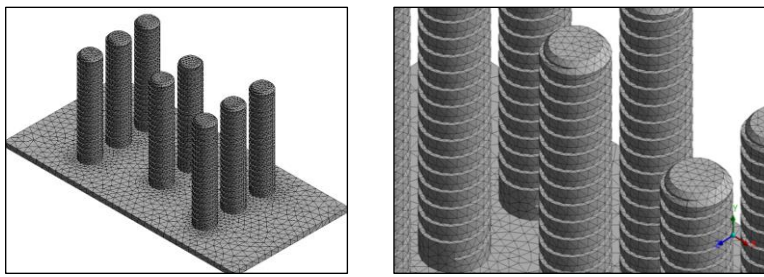

Figure 9: Meshing view of square threaded pin fin without perforation in a staggered arrangement

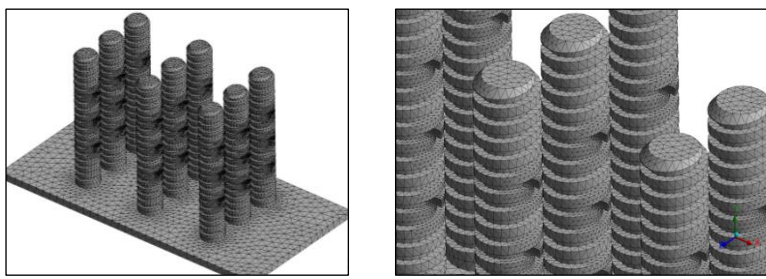

Figure 10: Meshing view of square threaded pin fin with perforation in inline arrangement

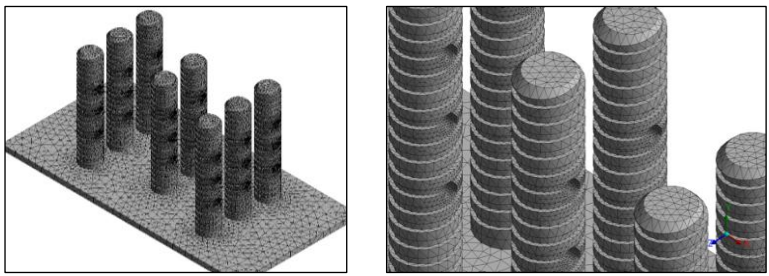

Figure 11: Meshing view of square threaded pin fin with perforation in a staggered arrangement

## Grid independent test

The grid independence test was carried out to determine the appropriate number and size of the elements in the simulation of this project. In this project, the size of elements was varied by decreasing the element size while keeping other simulation parameters constant. The test was carried out on a square threaded pin fin without perforation in inline arrangement with a heat flux at 15 W. Based on Table 3, the geometry of the domain was meshed using tetrahedral mesh algorithms after selecting the targeted physical parts to investigate heat transfer phenomena. The whole computational domain was tested with a different number of mesh element sizes ranging from 10 mm to 20 mm, then the average temperature value was plotted to check the acceptable grid size used as shown in Figure 12. The element size of 10 mm gave the highest number of elements with 4 514 282 which consumed very high time of the computational process. Since the difference in base temperature was not significant between mesh elements of 18, 16 and 13, the element size chosen was 13 mm because finer element size can increase the accuracy of results with better mesh quality.

Table 3: Summary of mesh independent test

| Element size (mm) | Mesh elements | Base temperature (K) | Fin temperature (K) |
|---|---|---|---|
| 20 | 2155645 | 364.3123 | 362.6670 |
| 18 | 3014229 | 364.5981 | 362.9528 |
| 16 | 3225512 | 364.5688 | 362.9235 |
| 13 | 3677634 | 364.5597 | 362.9144 |
| 10 | 4514282 | 364.6497 | 363.0056 |

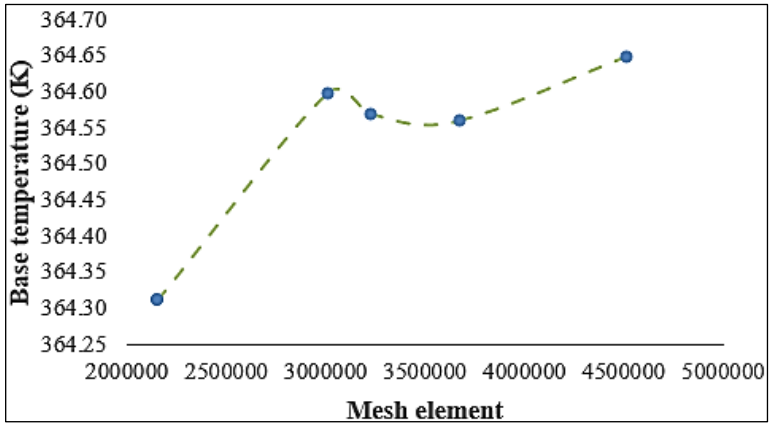


Figure 12: Mesh sensitivity analysis of grid independence test

## Governing equations

The governing differential equation for steady-state condition, laminar flow, constant property, and the three-dimensional flow with the incompressible ideal gas assumption is given by [21].
Continuity equation:

$$\frac{\partial u}{\partial x}+\frac{\partial v}{\partial y}+\frac{\partial w}{\partial z}=0 \tag{1}$$

Momentum equation:

$$\rho\left(U\frac{\partial U}{\partial x}+v\frac{\partial U}{\partial y}+w\frac{\partial U}{\partial z}\right)=\frac{\partial p}{\partial x}+u(\nabla^2 U) \tag{2}$$

$$\rho\left(u\frac{\partial v}{\partial x}+v\frac{\partial v}{\partial y}+w\frac{\partial v}{\partial z}\right)=-\frac{\partial p}{\partial y}+u(\nabla^2 v)-\rho g \tag{3}$$

$$\rho\left(u\frac{\partial w}{\partial x}+v\frac{\partial w}{\partial y}+w\frac{\partial w}{\partial z}\right)=-\frac{\partial p}{\partial y}+u(\nabla^2 w) \tag{4}$$

Energy equation:

$$u\frac{\partial T}{\partial x}+v\frac{\partial T}{\partial y}+w\frac{\partial T}{\partial z}=\alpha(\nabla^2 v) \tag{5}$$

At the pressure and temperature of the surroundings $P = P_{atm}$, $T = T_{\infty}$. The energy equation for conduction in solid $\nabla^2 T = 0$.

An assumption on the working fluid is air with incompressible ideal gas and properties of the fluid are measured at film temperature $T_{film} = (T_w + T_{\infty})/2$ where the $T_w$ is ambient temperature, and $T_{\infty}$ is the average surface temperature on the heat sink. Therefore, the result can be represented using the following non-dimensional parameters. Grashoff's Number is the ratio of buoyancy force to the viscous force acting in the fluid layer. The Grashoff number has the same importance in free convection as the Reynolds number in force convection to find the type of flow either laminar or transition turbulent in free convection [19]. The Grashoff number can be calculated as:

$$G_r = \frac{g \times \beta \times \Delta T \times z^3}{v^2} \tag{6}$$

where $g$ is the acceleration due to the earth's gravity, $z$ is the vertical length, $\beta$ is the coefficient of thermal expansion, $\Delta T$ is the temperature difference and $v$ is the kinematic viscosity For gases $\beta = 1/T$ where the temperature is in Kelvin. The Prandtl number is defined as the ratio of kinematic viscosity to thermal diffusivity. The Nusselt number is used to define the ratio of heat transfer by convection to the heat transfer by conduction within a fluid. Meanwhile, for natural convection, the equation for the Nusselt number can be calculated in the form of the Grashoff number and Prandtl number as,

$$Nu = 0.59(GrPr)^{0.25} \tag{7}$$

The heat transfer coefficient can be calculated as [20]:

$$h = \frac{N_u \times k}{z} \tag{8}$$

where $Nu$ is Nusselt number, $k$ is thermal conductivity and $z$ is vertical height.

## Results and Discussion

### Validation of simulation with experimental data from literature

Validation results of simulation are vital to ensure the accuracy and reliability of the simulation model against established data published in the literature. In this project, the heat sink simulation was validated against experimental data [16], which used a similar geometrical configuration and the same operating conditions. The detailed physical geometrical configuration of this study can be found in Table 1. The same geometry was adopted for simulation and tested

with a heat source of 15 W. Heat transfer coefficient was the main parameter for testing the validity of the simulation with experimental work using Equation (8). Table 4 shows the result for the heat transfer coefficient for both simulation and experimental.

Table 4: Validation result of heat transfer coefficient for pin fins in an inline and staggered array

| Heat transfer coefficient, h ($W/m^2K$) | Square threaded pin fin in inline pattern | Square threaded pin fin with perforation in inline pattern | Square threaded pin fin in staggered pattern | Square threaded pin fin with perforation in staggered pattern |
|---|---|---|---|---|
| Simulation | 7.38 | 7.24 | 7.27 | 7.46 |
| Experiment [16] | 7.32 | 7.46 | 7.65 | 7.83 |

Based on the result, validation of the heat transfer coefficient for numerical simulation and experimental results shows a good agreement in which the value is nearly the same. The percentage difference between numerical simulation and experiment results can be calculated using Mean absolute percentage error (MAPE). The MAPE formula is expressed as below:

$$MAPE = \frac{100}{N} \times \sum_{i=1}^{N} \left| \frac{x_i - \hat{x}_i}{x_i} \right| \quad (9)$$

where n, $x_i$ and $\hat{x}_i$ are the total numbers of value, simulation, and experimental values of the study respectively. Based on Table 5, the percentage errors are consistently less than 6%, therefore the present model is acceptable to predict the heat transfer coefficient of the heat sink.

## Analysis of heat transfer distribution on the heat sinks

Effect of fin pin arrangement and perforation on temperature distribution

Figures 13 to 16 show the temperature contours over the convective surface areas for pin fin heat sinks in inline and staggered arrays. From the observations, all the design models analysed show that the temperature distribution decreases gradually from the base plate to the length of the pin fins. In Figure 13, the base plate is characterized by shades of red and yellow, indicating that the initial temperature of the base plate is around 364.5 K, which is the hottest part of the heat sink. Along the pin fins, the colour shifts to blue, this gradually decreases the temperature of the pin fin from the base

plate to approximately 362.9 K. The temperature contour plot for Figure 10 reveals a consistent temperature gradient, indicating a gradual dissipation of heat from the base plate through the pin fins. This inline arrangement facilitates heat transfer but exhibits modest temperature reduction along the fins.

Table 5: MAPE error percentages between simulation and experimental results

| Heat sink | Square threaded pin fin in inline pattern | Square threaded pin fin with perforation in inline pattern | Square threaded pin fin in staggered pattern | Square threaded pin fin with perforation in staggered pattern |
|---|---|---|---|---|
| MAPE error % | 0.79 | 3.1 | 5.3 | 5.0 |

Figure 14 shows that the base plate is slightly cooler at the temperature of 360.1 K and the temperature decreases along the pin fins until the end of the pins at 358.7 K. Along the staggered pin fins, the colour gradually shifts toward dark blue tones for all pin fins. The heat dissipation in Figure 14 is slightly more efficient compared to Figure 13. The staggered arrangement introduces irregularities in the flow pattern, which contribute to improved cooling efficiency as indicated by the lower temperature at the end of the pin fins.

Figure 15 shows that the base plate temperature is 358.9 K, with the temperature decreasing to 357.2 K at the end of perforated pin fins. Comparison between Figures 13 and 15 shows that the addition of perforations to the pin fins in inline arrangement significantly increases heat dissipation from the heat flux at the base plate. This situation is predicted because an increase in effective heat transfer area enhances the rate of heat dissipation [22].

Figure 16 shows the result of a unique temperature distribution. The base plate temperature is relatively high at 367.6 K and the temperature decreases to 366.2 K at the end of the perforated pin fins. When comparing the colour trends in the temperature contour between Figure 15 and Figure 16 along the staggered pin fins, the colour gradually shifts toward dark blue tones for all pin fins in Figure 16. It shows that the threaded fin pins with perforation in staggered arrays are cooler and highly effective in dissipating heat, even though the base plate starts at a higher temperature. The colour trends in the temperature contour plots visualize how heat is distributed across the heat sink.

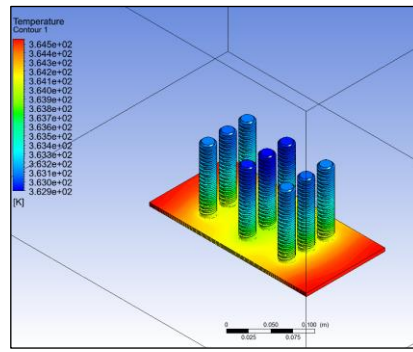


Figure 13: Temperature contour of inline pattern without perforation pin fins

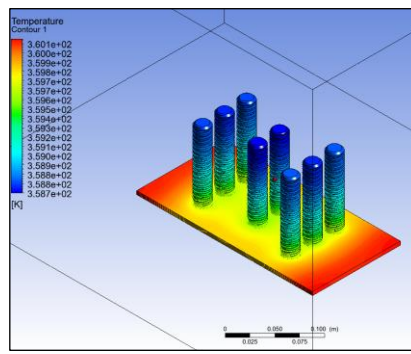


Figure 14: Temperature contour of staggered pattern without perforation pin fins

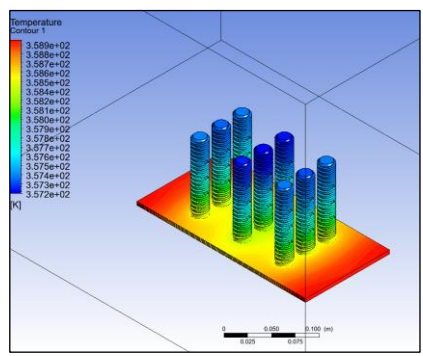


Figure 15: Temperature contour of inline pattern with perforation pin fins

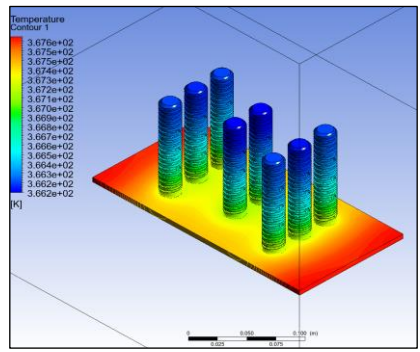


Figure 16: Temperature contour of staggered pattern with perforation pin fins

## Fluid flow visualization

Effect of fin pin arrangement and perforation on fluid flow

Figures 17 to 20 show the velocity vectors of the pin fin heat sink with variations in perforation and arrangement at 15 W heat input. These velocity vector plots offer critical insights into how these design factors impact the movement of air and consequently heat dissipation.

Figure 20 shows the high-velocity profile which indicates the presence of strong airflow and fluid turbulence. Vortex formations occur within this configuration. These vortices represent areas where the fluid flow separates from the pin fins and subsequently reattaches downstream. This flow separation and reattachment contribute to enhanced heat transfer by disrupting the thermal boundary layer near the heat sink surface. This phenomenon aligns with the findings [22] which highlight the potential of improved heat dissipation.

Figure 18 exhibits a lower-velocity profile compared to Figure 20. This lower-velocity profile is indicative of reducing fluid turbulence and weaker airflow within the pin fin array. The key distinction here is that the pin fins in this configuration lack perforations. Without perforations, the airflow is more obstructed by the pin fins, leading to lower circulation and higher resistance to flow. This increased resistance results in a higher-pressure loss within the pin fin structure [23].

A noteworthy observation from these velocity vector plots is the difference between inline and staggered arrangements. Staggered pin fins tend to allow for more unimpeded fluid flow between the fins, resulting in improved circulation and reduced flow blockages compared to inline arrangements. Consequently, staggered patterns tend to exhibit more favourable fluid flow characteristics for heat dissipation.

The role of perforations in pin fins becomes apparent when comparing Figures 18 (no perforations) and 20 (with perforations). Perforations disrupt

the flow near the pin fins, creating additional turbulence and enhancing mixing. This disruption leads to increased heat dissipation from the heat sink surface, a crucial factor in optimizing cooling efficiency.

Additionally, the fluid flow patterns in the inline pattern configurations, both with and without perforations, reveal a limitation. The pin fins in the middle of the inline pattern receive insufficient airflow to dissipate heat effectively. This is attributed to the sequential arrangement of pin fins, where air struggles to rise parallel through the fins. As a result, this configuration might experience reduced heat transfer performance.

In summary, these fluid flow visualizations provide valuable insights into the impact of perforations and pin fin arrangement on heat sink performance. Perforations disrupt flow and enhance turbulence, while staggered arrangements generally promote more efficient fluid circulation. Understanding these flow patterns is critical for optimizing heat sink designs, ensuring effective heat dissipation, and maintaining safe operating temperatures for electronic devices. This analysis underscores the importance of design choices in achieving superior thermal management.

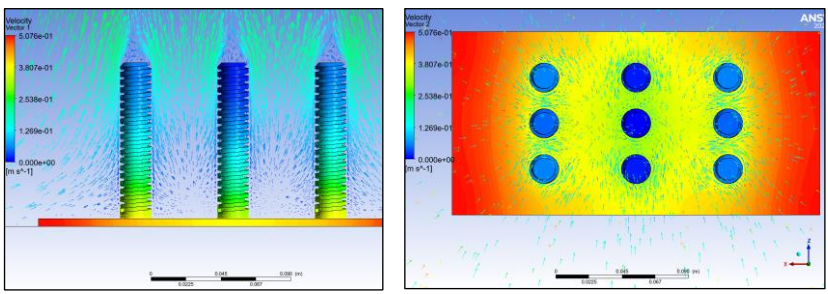

(a) xy-plane (b) yz-plane

Figure 17: Air flow velocity profile of inline pattern without perforation

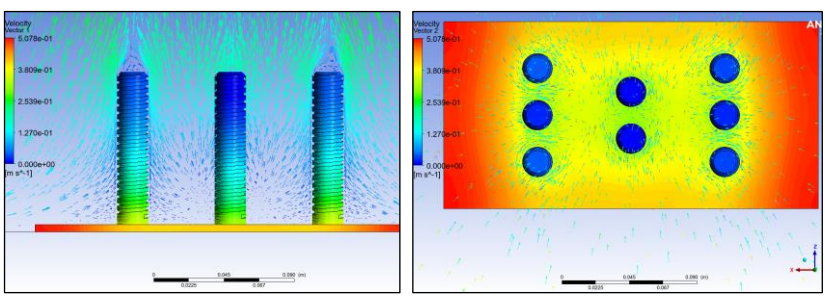

(a) xy-plane (b) yz-plane

Figure 18: Air flow velocity profile of staggered pattern without perforation

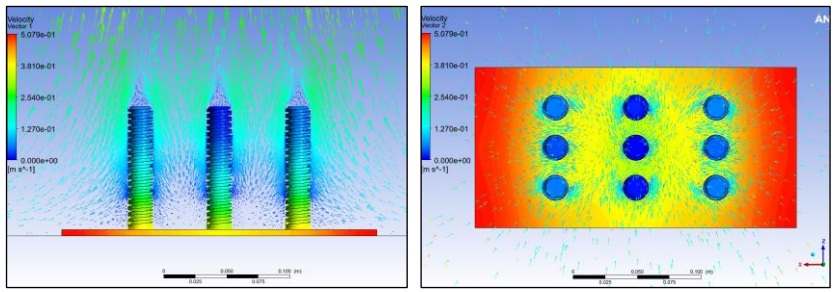


(a) xy-plane (b) yz-plane

Figure 19: Air flow velocity profile of inline pattern with perforation

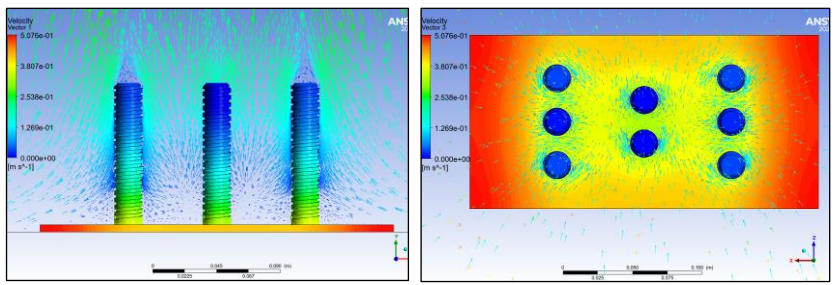


(a) xy-plane (b) yz-plane

Figure 20: Air flow velocity profile of staggered pattern with perforation

## Thermal performance

In Figure 21, the graph presents a linear trend in the relationship between the resulting temperature difference *(ΔT)* and the power input applied to the base plate of the heat sink for four distinct pin fin configurations. When power input increases, the temperature difference also tends to increase. This correlation reflects the basic principle that higher heat loads lead to greater temperature differentials within the heat sink.

Pin fins with perforation in the staggered pattern have a higher temperature difference followed by pin fins in inline pattern. The higher temperature difference measured at the base plate with the temperature at atmospheric air is due to the arrangement in the staggered pattern which can reduce the obstruction for the fluid to flow through the entire pin fins. Thus, a more convective surface area actively dissipates heat to the surrounding air [24]. This configuration is the most effective in dissipating heat.

The Rayleigh number is a dimensionless number that quantifies the relative effects of buoyancy and viscous forces in fluid flow. It is a critical parameter in natural convection heat transfer. Meanwhile, the Nusselt number

represents the ratio of convective heat transfer to conductive heat transfer in a fluid. It characterizes the effectiveness of heat transfer, with higher *Nu* values indicating more efficient cooling.

For all configurations of pin fin, there is a positive correlation between *Nu* and *Ra* as shown in Figure 22. This means that as the Rayleigh number increases, the Nusselt number also tends to increase. This relationship is in line with the expectations in natural convection, where higher *Ra* values typically lead to enhanced convective heat transfer [24]. Pin fins with perforation in the staggered pattern have the highest Nusselt number while pin fins with perforation in inline pattern have the lowest Nusselt number. The difference between the highest Nusselt number of pin fins in staggered with perforation and the second highest pin fins in inline pattern is about 0.62%. The combination of staggered patterns and perforations promotes more effective convective cooling.

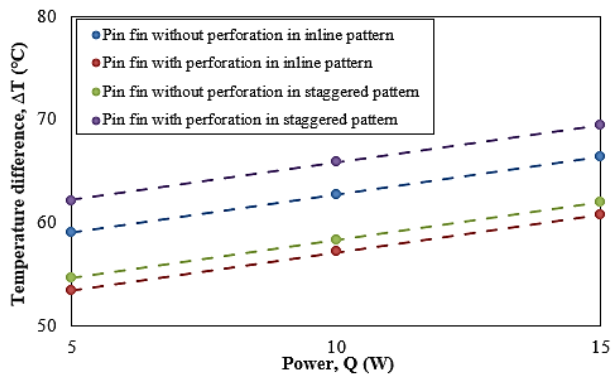


Figure 21: Temperature differences, $\Delta T$ against the power input, $Q$

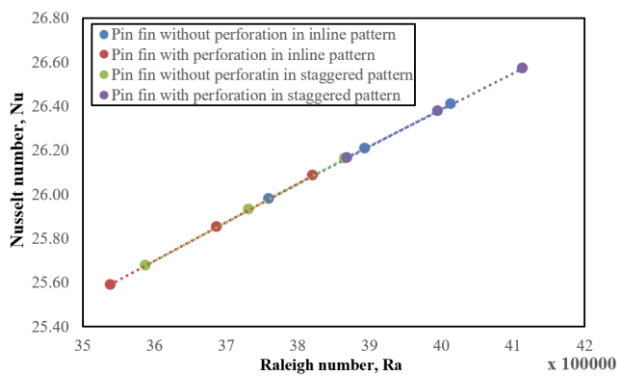


Figure 22: The relation of Nusselt number, *Nu* and Rayleigh number, *Ra*

From Figure 23, all the models showed the same trend as Figure 22 which indicates a positive correlation between Nusselt number, *Nu* and heat transfer coefficient, *h*. Higher Nusselt numbers typically indicate more efficient heat transfer, while the heat transfer coefficient quantifies the rate of heat exchange between a solid surface and a fluid. Lower Nusselt numbers reduce convective heat transfer, which is often associated with laminar flow or less effective heat dissipation. The positive correlation between *Nu* and h is essential for engineers and researchers in the field of thermal management. It implies that by optimizing the pin fin configuration and geometry to achieve higher Nusselt numbers, the heat transfer performance of a heat sink can be enhanced, resulting in more efficient cooling of electronic devices. These findings can be valuable in designing heat sinks for various applications where effective heat dissipation is crucial. From both graphs, it can be stated that pin fins with perforation in staggered patterns have better thermal performance than the other model of heat sink.

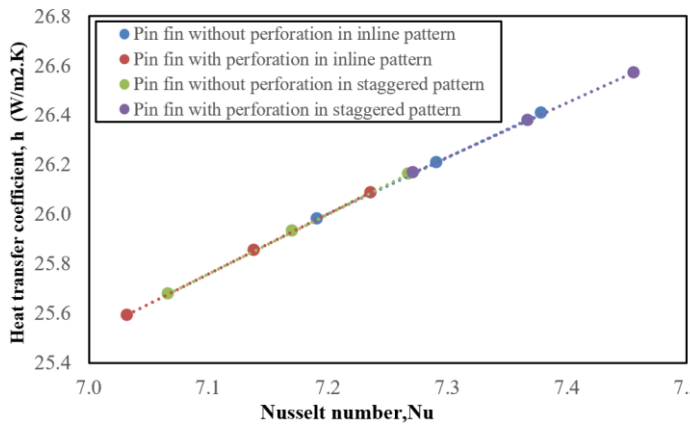


Figure 23: The relation of heat transfer coefficient, *h* and Nusselt number, *Nu*

Figure 24 shows that the heat transfer coefficient tends to increase with higher power inputs across all square threaded pin fins. This behaviour is consistent with the expected response of convective heat transfer, where higher power inputs lead to greater temperature gradients and increased heat dissipation. Pin fins with perforation in the staggered pattern have the highest heat transfer coefficient at each power supply while pin fins with perforation in inline pattern have the lowest heat transfer coefficient. For the square threaded pin fin in the staggered pattern with perforation, the result demonstrates a consistent rise in the heat transfer coefficient as power input increases. This model offers the highest heat transfer coefficients, making it a promising choice for applications with high power densities. As a comparison,

the average difference between *h* of the pin fin with perforation and the pin fin without perforation in the staggered pattern is 2.75%. Therefore, the pin fin with perforation in a staggered pattern dissipates heat at the rate of 2.75% more than the pin fin without perforation.

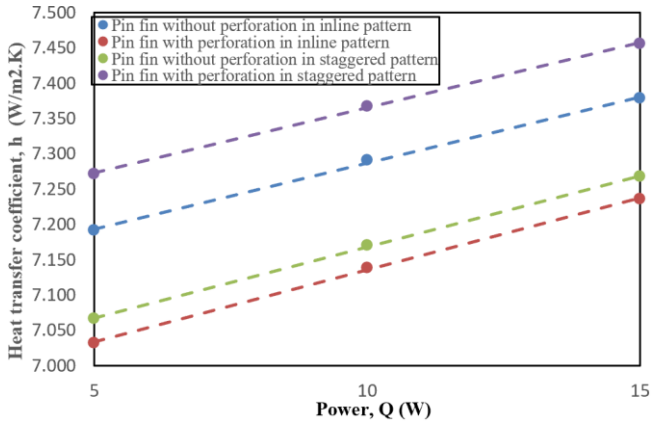


Figure 24: The relation of heat transfer coefficient, *h* and power input, Q

## Conclusion

This project presents a numerical analysis for the investigation of flow patterns and quantifies the heat transfer characteristics of the square threaded pin fins integrated into the heat sink by natural convection. Four configurations were analysed based on the pin fins with or without perforations in an inline or staggered pattern. The effects of different arrangements and the presence of perforations, all under the conditions of natural convection, were analysed. The simulation was validated with previous studies to determine the heat transfer coefficient, *h*. In this project, the result for validating the Ansys CFD simulation with the experiment [16] shows about a 5% error of heat transfer coefficient for square threaded pin fins with perforation in a staggered pattern. Temperature contours reveal that all design models exhibit a gradual decrease in temperature from the base plate to the end of the pin fins. While the inline arrangements facilitate heat transfer, the staggered arrangements, especially those with perforations, demonstrate more efficient heat dissipation. This shows that the choice of pin fin arrangement plays a pivotal role in thermal performance. The additional perforations in inline arrangements significantly increase heat dissipation by expanding the effective heat transfer area. Threaded fin pins with perforations in staggered patterns prove to be highly effective in dissipating heat, despite a relatively higher base plate temperature.

The colour trends in the temperature contour plots vividly depict how heat is distributed across the heat sink. The enhancement in heat dissipation rate due to perforation is noted when having a higher contact surface with fluid in comparison with the pin fins without perforation. The extended effective surface area with the application of threaded geometry on pin fins contributes a good medium of convection heat transfer. The fluid flow visualization elucidates the relationship between pin fin patterns, perforations, and airflow patterns. Staggered pin fin pattern disrupts the flow less, resulting in improved circulation and reduced flow blockages compared to inline arrangements. Perforations introduce turbulence and enhance mixing, contributing to increased heat dissipation. For thermal performance, as power input increases, temperature differences also tend to rise. The higher heat loads lead to greater temperature differentials within the heat sink. Thus, a more convective surface area actively dissipates heat to the surrounding air. The threaded fin pins with perforations in staggered patterns are the most effective in dissipating heat. The heat transfer coefficients increase with higher power inputs. Pin fins with perforations in staggered patterns consistently offer the highest heat transfer coefficients, making them particularly attractive for applications with elevated power densities. In summary, this research project significantly contributes to the understanding of thermal management through square-threaded pin fins. By optimizing pin fin arrangements and introducing perforations, the square-threaded pin fins have higher heat transfer performance than others. These findings hold substantial implications for the design and engineering of heat sinks in a wide range of electronic applications.

## Contributions of Authors

The authors confirm the equal contribution in each part of this work. All authors reviewed and approved the final version of this work.

## Funding

This work was supported by the “Geran Penyelidikan Khas” from Universiti Teknologi MARA (UiTM) [600-RMC/GPK 5/3 (133/2020)].

## Conflict of Interests

One of the authors, Rosnadiah Bahsan, is an assistant managing editor of the Journal of Mechanical Engineering (JMechE). The author has no other conflict of interest to note.

## References


[1] M. Tejas Sonawane, M. Prafulla Patil, M. A. Chavhan, B. M. Dusane, and Nashik. Management, "A review on heat transfer enhancement by passive methods," *International Research Journal of Engineering and Technology*, vol. 3, no. 9, pp. 1567-1574, 2016.

[2] A. Al-Damook, N. Kapur, J. L. Summers, and H. M. Thompson, "An experimental and computational investigation of thermal air flows through perforated pin heat sinks," *Applied Thermal Engineering*, vol. 89, pp. 365–376, 2015. https://doi.org/ 10.1016/j.applthermaleng.2015.06.036

[3] A. S. Nathan, R. S. Silson, M. Syed Kani, G. U. Pandian, and U. Nainar, "Performance enhancement of minichannel heat sink," *International Journal of Innovative Research in Science*, vol. 8, no. 3, pp. 3201-3211, 2019. https://doi.org/ 10.15680/IJIRSET.2019.0803226

[4] H. E. Ahmed, B. H. Salman, A. S. Kherbeet, and M. I. Ahmed, "Optimization of thermal design of heat sinks: A review," *International Journal of Heat and Mass Transfer*, vol. 118, pp. 129–153, 2018. https://doi.org/10.1016/j.ijheatmasstransfer.2017.10.099.

[5] V. Choudhary, M. Kumar, and A. K. Patil, "Experimental investigation of enhanced performance of pin fin heat sink with wings," *Applied Thermal Engineering*, vol. 155, no. 9, pp. 546-562, 2019. https://doi.org/10.1016/j. applthermaleng.2019.03.139.

[6] Y. Joo, and S. J. Kim, "Comparison of thermal performance between plate-fin and pin-fin heat sinks in natural convection," *International Journal of Heat and Mass Transfer*, vol. 83, pp. 345-356, 2015. https://doi. org/10.1016/j.ijheatmasstransfer.2014.12.023

[7] X. Meng, J. Zhu, X. Wei, X., and Y. Yan, "Natural convection heat transfer of a straight-fin heat sink," *International Journal of Heat and Mass Transfer*, vol. 123, pp. 561-568, 2018. https://doi.org/10.1016/j. ijheatmasstransfer.2018.03.002

[8] S. A. Nada, and M. A. Said, "Effects of fins geometries, arrangements, dimensions and numbers on natural convection heat transfer characteristics in finned-horizontal annulus," *International Journal of Thermal Sciences*, vol. 137, pp. 121-137, 2019. https://doi.org/10.1016/j.ijthermalsci.2018.11.026

[9] M. R. Haque, T. J. Hridi, and M. M. Haque, "CFD studies on thermal performance augmentation of heat sink using perforated twisted, and grooved pin fins," *International Journal of Thermal Sciences*, vol. 182, no. 6, p. 107832, 2022. https://doi.org/10.1016/j.ijthermalsci.2022.107832

[10] G. Song, D. H. Kim, D. H. Song, J. bin Sung, and S. J. Yook, "Heat-dissipation performance of cylindrical heat sink with perforated fins,"

*International Journal of Thermal Sciences*, vol. 170, p. 107132, 2021. https://doi.org/10.1016/j.ijthermalsci.2021.107132

[11] A. Maji, D. Bhanja, and P. K. Patowari, "Numerical investigation on heat transfer enhancement of heat sink using perforated pin fins with inline and staggered arrangement", *Applied Thermal Engineering*, vol. 125, pp. 596–616, 2017. https://doi.org/ 10.1016/j.applthermaleng.2017.07.053

[12] P. Laad, B. Akhare, and P. Chaurasia, "Thermal analysis of heat sink with fins of different configuration using ANSYS workbench 14.0," *International Journal of Engineering Sciences & Research Technology*, vol. 5, no. 6, pp. 82-93, 2016. https://doi.org/10.5281/zenodo.54668

[13] A. Harry Richard T. L., "Experimental analysis of heat transfer enhancement using fins in pin fin apparatus," *International Journal of Core Engineering & Management*, vol. 2, no. 1, pp. 123-132, 2015.

[14] S. Bakre, A. Arya, and B. M. Rathore, "Study of thermal hydraulic performance of various pin fin heat sink by using computational fluid dynamics," *International Journal for Scientific Research & Development*, vol. 3, no. 1, pp. 499-506, 2015.

[15] S. Sharbuddin Ali, "Experimental study on heat sink using screw thread," *International Journal of Innovative Science and Research Technology*, vol. 2, no. 12, pp. 26-34, 2017.

[16] B. Olekarp and G. Tp, "Experimental and numerical analysis of cylindrical pin fins having square thread with and without perforations by natural and forced convection," *International Journal of Innovative Science, Engineering & Technology*, vol. 3, no. 7, pp. 512-516, 2016.

[17] S. T and S. K. D, "Heat transfer study on different surface textured pin fin heat sink," *International Communications in Heat and Mass Transfer*, vol. 119, p. 104902, 2020. https//doi.org/10.1016/j.icheatmasstransfer.2020.104902

[18] Perry, J, "Thermal comparison of copper and aluminum heat sinks" 28 March 2017. [Online] Available: https://www.qats.com/cms/2017/03/28/case-study-thermal comparison-copper-aluminum-heat-sinks/ (Accessed 20 April, 2022)

[19] Zagala, E. J., "Heat conductivity", in B. Bhushan (Ed.), Encyclopedia of Nanotechnology, Springer, 2016, pp. 1453-1453, https://doi.org/10.1007/978-94-017-9780-1_100385

[20] D. Hanamant, K. N. Vijaykumar, and D. Kavita, "Natural convection heat transfer flow visualization of perforated fin arrays by CFD simulation," *International Journal of Research in Engineering and Technology*, vol. 2, no. 12, pp. 483-490, 2013. https://doi.org/10.15623/ijret.2013.0212081

[21] R. Siddhardha, S. Bhatti, P. Subramanyam, and A. Professor, "Numerical investigation on heat transfer enhancement by Natural Convection with

Perforated Fins," *International Journal of Research and Analytical Reviews*, vol. 5, no. 4, pp. 693-699, 2018.

[22] A. Naufal bin Samsudin, A. Salami Tijani, S. Thottathil Abdulrahman, J. Kubenthiran, and I. Kolawole Muritala, "Thermal-hydraulic modeling of heat sink under force convection: Investigating the effect of wings on new designs," *Alexandria Engineering Journal*, vol. 65, pp. 709-730, 2023. https://doi.org/ 10.1016/j.aej.2022.10.045

[23] Y. Yan, T. Zhao, Z. He, Z. Yang, and L. Zhang, "Numerical investigation on the characteristics of flow and heat transfer enhancement by micro pin-fin array heat sink with fin-shaped strips," *Chemical Engineering and Processing - Process Intensification*, vol. 160, no. 1, p. 108273, 2021. https://doi.org/ 10.1016/j.cep.2020.108273

[24] A. S. Tijani and N. B. Jaffri, "Thermal analysis of perforated pin-fins heat sink under forced convection condition," *Procedia Manufacturing*, vol. 24, pp. 290–298, 2018. https://doi.org/ 10.1016/j.promfg.2018.06.025